A NEW AND FUNDAMENTAL EXPERIMENT ON TOTAL REFLECTION

F. Goos and H. Hänchen

Annalen der Physik 1, 333-346 (1947)

Translated at CERN by J. Nicholls
(Original: German)
Revised by H. MacCabe

(CERN Trans. 72-3)

Geneva
January 1972

HM/ms

A New and Fundamental Experiment on Total Reflection

by F. Goos and H. Hänchen

(with 11 figures)

Note : All Footnotes are found at the end of the text.

(Translated from : Annalen der Physik, 6. Folge, Band 1,1947)

Summary

According to Maxwell's theory, light energy penetrates into the less dense medium whenever total reflection occurs. Experimentally, this penetration has so far always been demonstrated only in the less dense medium itself ; in doing so, light was drained off, so that the reflection was no longer total. This paper describes a new experiment in which the movement of the light in the less dense medium is ascertained by means of a phenomenon experienced in the denser medium after the light has already passed through and out of the less dense one. Hence, total reflection is not interfered with in any way. The phenomenon is quantitatively related to Maxwell's theory.

---

§ 1. Introduction and Historical Survey

The theory of total reflection, as derived from Maxwell's equations, states that such reflection does not take place abruptly at the boundary surface between the optically denser and the optically less dense media, but that the energy penetrates a short distance into the less dense medium before the process of total reflection occurs.

The detailed behaviour of the energy flow in the less dense medium has been discussed many times on the basis of Maxwell's theory [1]. It has been found that the energy moves along the boundary ; that, within the less dense medium, it has perceptible values only in the immediate vicinity of this boundary, and shows a rapid, exponential decrease at right angles thereto, representing a transversely attenuated wave. The most remarkable feature of this process is that the light energy flows from the denser into the less dense medium at certain points, and returns again in undiminished strength to the denser medium at another point, so that we are justified in regarding the reflection as total.

Many researchers, beginning with Newton some 250 years ago, have furnished experimental proof of the presence of light energy in the less dense medium during total reflection [2]. However, among all these experiments and their many variants there is not a single one in which the flow of energy in the less dense medium has not been interfered with in some way, primarily for the reason that it is, in fact, impossible to demonstrate the presence of energy without draining some of it away, so that the totality of the reflection is destroyed. Therefore, at first glance, it does not seen possible that an experiment can be devised which allows the light energy in the less dense medium to be detected while total reflection is completely maintained.

The experiments in which total reflection is destroyed [3] will not be described here in detail : the so-called "lamination experiment" in particular has been the subject of extensive discussion, since it provides the most accurate quantitative proof of Maxwell's theory. It has recently been performed by us in a comprehensive manner using photographic-photometric means[4]. The Voigt experiment[5], in which a prism

with a slight kink in its hypotenuse surface is used, is also very worthly of note, as is the Selényi one [6], although it likewise seems to suffer from the disadvantage of interfering with the propagation of the light in the less dense medium.

§ 2. A Novel Approach to the Problem and its Experimental Implementation

The purpose of this paper is to describe a novel experiment in which there is not the slightest interference with the movement of the light in the less dense medium. In particular, no energy at all is tapped off, so that the process of total reflection remains undisturbed. Nevertheless, this experiment furnishes irrefutable proof of the penetration of the light into the less dense medium ; moreover, it allows Maxwell's theory to be subjected to a quantitative check.

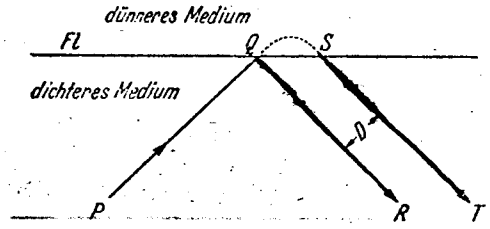

Fig. 1 : Principle of the ray path.
dünneres Medium = less dense medium
dichteres Medium = denser medium

The experiment is based on the theoretical prediction that the light energy enters the less dense medium at certain points of the boundary, and returns at others in undiminished strength.

The decisive experiment is outlined below in a simplified form.

In fig. 1., Fl represents the boundary surface between the optically dense and optically less dense media ; it is perpendicular to the plane of the page. A ray of light PQ impinges upon it at an angle within the total reflection range. If total reflection were to take

place directly at the boundary at point Q, the totally reflected light ray would follow path QR ; if, however, the ray first enters the less dense medium as predicted by Maxwell's theory, it will leave it again roughly at point S and travel along path ST. No assumptions at all are made about the movement of the light inside the less dense medium which is represented in fig. 1 by the broken line between Q and S.

Although it is not possible to use in the experiment a single "ray" of light, but only a narrow beam with a certain, albeit very small angle of aperture, the phenomenon described will, nevertheless, occur : the initially imagined ray QR will be subject to a displacement D and cause the actual ray ST to appear.

The question now is whether it is possible :

- firstly, to produce the notional ray QR in the experiment and thus render the ray displacement D visible and measurable ;
- secondly, to measure this obviously very small displacement with sufficient accuracy.

We managed to do both by the following method :

1. Production of the ray QR (fig. 1) : this was accomplished by the use of metal films, e.g. a film of silver, applied to glass. In the yellow/red range of the spectrum, a film of silver only about 50 m/u thick reflects already 95 % of the incident light fairly independently of the angle of incidence. Because of the high absorption coefficient of silver, the light striking the silver film can penetrate it only to an exceedingly small extent - - estimated at a few m/u --, being forced back, i.e. reflected, already in the very topmost layers. The depth of penetration into the silver is certainly less than 1 % of the depth which one may expect for total reflection (i.e. when the light penetrates into the less dense medium)

and which will be of the order of magnitude of a few wavelengths (i.e. of the order of magnitude of 1000 m/u).

If, therefore, boundary F1 in fig. 1 were silvered, ray PQ would be reflected practically at point Q, and ray QR would appear.

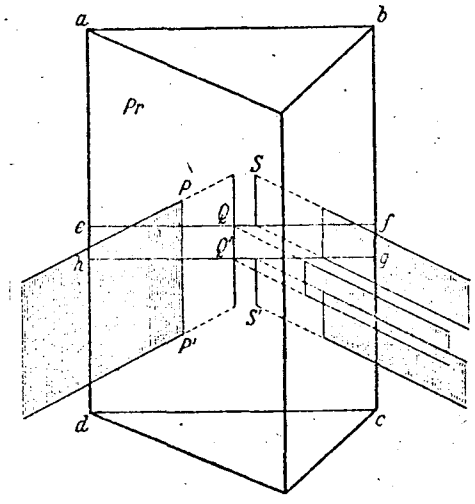

Fig. 2 :
Production of the ray

In the actual experiment, a strip of silver is applied to the surface of the glass at which total reflection is to take place, as shown in fig. 2.

Pr is a glass prism ; total reflection occurs at its rear surface abcd. Part of this surface, strip efgh, is silvered. At PP',

a narrow beam of light (shown hatched) enters the prism. That part of it which strikes the silver strip is directly reflected at incidence QQ' ; above and below, the light is totally reflected at the glass/air boundary and leaves the less dense medium only at SS'. The narrow light beam, which has thus been divided into three parts, is captured by a photographic plate where it leaves a track as shown in fig. 3. In this way, the displacement D of the ray can be directly observed.

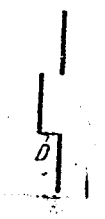

Fig. 3
Ray displacement

2. Of course, this displacement D will be very small (order of magnitude : the length of a light wave) ; hence, at first sight, its measurement would appear to be impossible. The effect can, however, be magnified without any difficulty by multiplying the reflections by means of a plane-parallel glass plate, as shown in fig. 4.

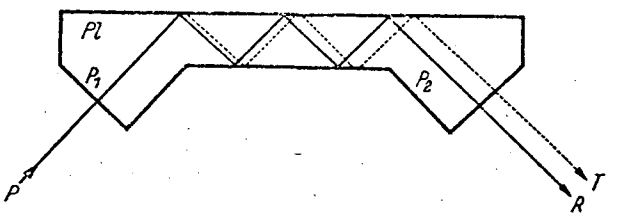

Fig. 4 : Principle of multiple reflection

Pl is a long, thin, plane-parallel glass plate with a suitable silver strip on one or, as in fig. 4, on both of its sides. Two right-angled prisms P_1 and P_2 are secured with oil to the ends of the plate to provide entry and exit points for the light. The path of the ray PR is shown as

a solid line, and that of ray PT as a broken line. The number of reflections and hence the magnification of the displacement cannot be increased at will, since only some 95% of the incident light is reflected from the silver (ray PR), so that, with repeated reflection, the reflected ray becomes progressively weaker. Nevertheless, it was possible to reflect the ray off the silver up to a maximum of about seventy times, after which the intensity of the reflected light was still $(0.95)^{70} = 0.028$, or not quite 3% of the incident light. The process of multiple reflection did, however, make it possible for the displacement D to be perceived by the naked eye and measured with considerable accuracy (see § 4).

3. A modified form of the experiment will now be described. It will be obvious that the displacement D will increase with the wavelength of the light, so that there will be a differential displacement between light of different colours (e.g. $\lambda = 0.578\,\mu$ and $\lambda = 0.435\,\mu$). This displacement will be very small, corresponding to a wavelength difference $\Delta\lambda = 0.143\,\mu$, but, needing no zero ray, this measurement will not require a silver film either, so that the only phenomenon used will be that of total reflection. In this way, the number of reflections can be increased considerably without any appreciable loss of light. We succeeded in measuring this slight differential effect with sufficient accuracy, especially as we had arranged the experimental set-up in such a way that the actual quantity measured was twice the differential ray displacement, i.e. $2 \cdot \Delta D$.

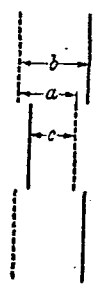

Fig. 5 :
Ray displacement for
the differential method

This was accomplished in the following way : consecutively, either the upper and lower parts or the central part of the narrow incident beam of light (see fig. 2) could be masked off at will. First of all, blue light was used for the upper and lower parts and yellow light for the central part, and the image of the reflected beam recorded on a photographic film ; then, the film was shifted through an arbitrary distance a and the light track photographed once more, but this time with yellow light above and below and blue light in the middle.

In fig. 5, the yellow track is shown as a solid line and the blue as a broken line.

The distances b and c were measured ; $2\Delta D = b - c$. The distance a through which the film was shifted is eliminated when the difference is calculated.

Having outlined the underlying principles, the detailed construction of the apparatus will now be described.

§ 3. The Experimental Layout

The experimental lay-out featured a Schmidt & Haensch spectrometer, the vernier scale of which gave readings to an accuracy of 30".

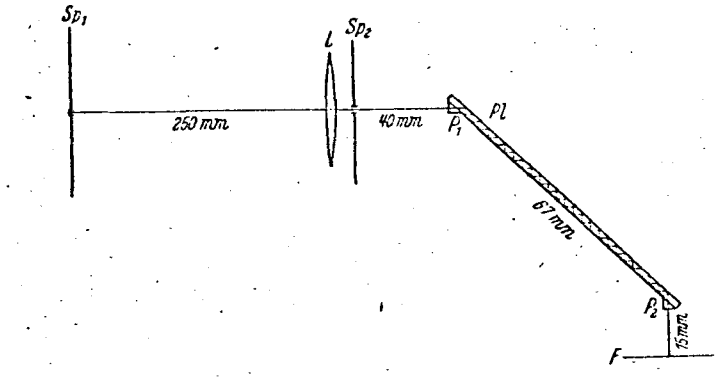

Fig. 6: Experimental Layout

The focal length of the collimator lens (fig. 6) was 250 mm. The slit Sp_1 at the focal point of the collimator lens was 0.20 mm wide and 0.5 mm high. A second long slit Sp_2, set at 0.30 mm width, was fitted behind the collimator lens L. With the aid of condenser lenses, yellow, green and blue light from a mercury lamp - or, for purposes of adjustment, red-filtered light from an arc - could be directed at will on to slit Sp_1, emerging, in accordance with both slits, as a narrow beam some 0.3 mm wide which then impinged on the reflection plate Pl (see also fig.4). The useful length of the plate Pl was 67 mm; as to thickness, 0.5, 1, or 2 mm were used. A test showed that the beam had an aperture angle of about 3' and that the intensity decreased rapidly in the lateral direction.

The film F was always perpendicular to the direction of the incident ray.

A rotating sector was fitted directly behind slit Sp_2 to ensure that the density of the various parts of the light tracks on film F (see figs. 3 and 5) was as nearly as possible uniform. In addition,

there was a diaphragm device directly in front of film F which allowed the yellow and blue light (see fig. 5) to be sharplymasked off in accordance with the requirements of the differential method (see § 2, No. 3).

The multiple reflections in plate P1 were obtained not only at the glass/air but also, when desired, at the glass/water boundary. This was achieved by making provision for a layer of water to be sucked up by capillary action on to that side of plate P1 to which the silver strip had also been applied. Otherwise, the silver strips were applied in part to one side and in part to both sides of plate P1 by cathodic sputtering and their reflectance measured (more detailed information on this may be found in reference 7).

For checking purposes, a silvered strip was sometimes applied above and below, while the central strip was left blank.

Mostly, the light tracks on film F (it was possible to make a number of consecutive exposures by shifting the film laterally) were measured with a measuring microscope. When the differential method was used (see 2, No. 3), a projection at 50 times magnification was also employed, allowing direct measurements to be made on the enlarged image with the aid of a millimetre rule. It was rather difficult to measure the lines, since the definition and particularly the shapes of the light tracks had suffered somewhat because of the multiple reflections; the tracks associated with total reflection had suffered more than those produced by the light reflected from the silver. This is because some of the quality is invariably lost through diffusion, however clean the reflection plate may be. The polishing, too, must be immaculate and the plates must be properly plane parallel (interference plates).

§ 4. The Measurements

Fig. 7 illustrates the displacement V in air after one reflection; V is obtained by dividing the displacement G actually measured by the number Z of effective reflections, i.e. $V = \frac{G}{Z}$. The displacement D in glass, i.e. in the denser medium, which alone is of interest here, is given by

$$D = V \frac{\cos \beta'}{\cos \alpha'} = \frac{G}{Z} \frac{\cos \beta'}{\cos \alpha'},$$

in accordance with the refraction by prism P_2.

For the photographs pertaining to total reflection from water, the factor $\frac{\cos \beta'}{\cos \alpha'}$ has the following values:

Photographs:

No. 67-69 (see table 2 below) . . . . . $\frac{\cos \beta'}{\cos \alpha'} = 1.075$

No. 70-71 . . . . . = 1.070

No. 72-73 . . . . . = 1.068

For all other photographs, i.e. for those which pertain to total reflection from air, this factor equals 1, within the limits of the accuracy of measurement.

It should also be pointed out that in the differential exposures ($\lambda = 0.578/u$ against $\lambda = 0.435/u$), i.e. in photographs No. 11-23 (see table 3), ray PQ always entered prism P_1 at an angle of exactly 90° (hence $\alpha = \beta = 0$) in order to avoid any dispersion and falsification of the differential displacement effect. Since the angle γ of prism P_1

was 44° 37.5' and the angle δ of prism P_2 44° 45.5' (i.e. since both were nearly 45°), the rays QR and ST left the prism P_2 at an angle so close to 90° that there was no appreciable dispersion effect there either.

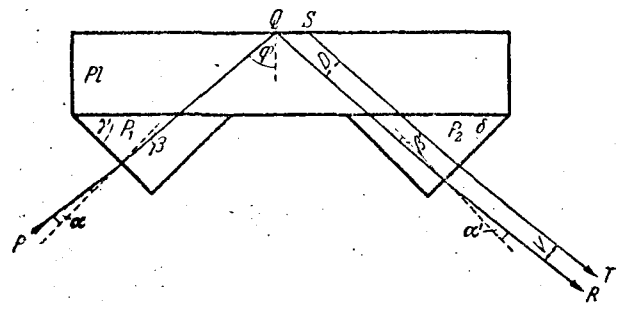

Fig. 7: Actual ray paths

The refractive indices of the two prisms P_1 and P_2, of the three plates used and of the film of water (at 20°C) are given in table 1 together with the critical angles φ_c of total reflection ($\sin \varphi_c = \frac{n_2}{n_1}$).

Table 1

	$\frac{n_2}{n_1}$			φ_c		
	$\lambda_{Vac} = 0{,}578\ \mu$	$\lambda_{Vac} = 0{,}546\ \mu$	$\lambda_{Vac} = 0{,}435\ \mu$	$\lambda_{Vac} = 0{,}578\ \mu$	$\lambda_{Vac} = 0{,}546\ \mu$	$\lambda_{Vac} = 0{,}435\ \mu$
Prisma P_1 und P_2 geg. Luft	$\frac{1}{1{,}5171}$	$\frac{1}{1{,}5187}$	$\frac{1}{1{,}5268}$	—	—	—
Platte ½ mm dick geg. Luft	$\frac{1}{1{,}5175}$	$\frac{1}{1{,}5192}$	$\frac{1}{1{,}5272}$	41° 13′, 3	41° 10′, 0	40° 54′, 2
Platte 1 mm dick geg. Luft	$\frac{1}{1{,}5170}$	$\frac{1}{1{,}5187}$	$\frac{1}{1{,}5267}$	41° 14′, 2	41° 10′, 9	40° 55′, 2
Platte 1 mm dick geg. Wasser	$\frac{1{,}3333}{1{,}5170}$	$\frac{1{,}3344}{1{,}5187}$	$\frac{1{,}3403}{1{,}5267}$	61° 30′, 6	61° 29′, 0	61° 23′, 5
Platte 2 mm dick geg. Luft	—	$\frac{1}{1{,}5105}$	—	—	41° 27′, 3	—

Prisma P_1 und P_2 geg. Luft = Prisms P_1 and P_2 to air

Platte ½ mm dick geg. Luft = ½ mm plate to air

Platte 1 mm dick geg. Luft = 1 mm plate to air

Platte 1 mm dick geg. Wasser = 1 mm plate to water

Platte 2 mm dick geg. Luft = 2 mm plate to air.

Table 2

1	2	3	4	5	6	7	8	9	10	11
Nr. der Aufnahme	Art der Aufnahme	benutzte Hg-Linie λ_{vac}	φ	$\varphi - \varphi_a$	G	Z	D	$\frac{D}{\lambda_1}$	$\sqrt{\sin^2\varphi - \left(\frac{n_2}{n_1}\right)^2}$	Gruppe
27	1 mm Platte S—G an Luft c	0,578 μ	44°37',4	3°23',2	48,0 μ	34	1,41 μ	3,70	0,2427	
28	1 mm Platte S—G an Luft e	0,578 μ	44°37',4	3°23',2	42,5 μ	34	1,25 μ	3,28	0,2427	
29	1 mm Platte S—G an Luft e	0,578 μ	44°37',4	3°23',2	21,0 μ	34	0,62 μ	1,62	0,2427	
30	1 mm Platte S—G an Luft e	0,578 μ	44°37',4	3°23',2	38,0 μ	34	1,12 μ	2,94	0,2427	
32	1 mm Platte S—G an Luft e	0,578 μ	44°37',4	3°23',2	13,0 μ	34	0,38 μ	1,00	0,2427	
33	1 mm Platte S—G an Luft e	0,578 μ	44°37',4	3°23',2	17,3 μ	34	0,51 μ	1,34	0,2427	
34	1 mm Platte S—G an Luft e	0,578 μ	44°37',4	3°23',2	28,8 μ	34	0,85 μ	2,22	0,2427	I
36	1 mm Platte S—G an Luft e	0,578 μ	44°37',4	3°23',2	35,6 μ	34	1,05 μ	2,74	0,2427	
37	1 mm Platte S—G an Luft e	0,578 μ	44°37',4	3°23',2	27,0 μ	34	0,79 μ	2,08	0,2427	
38	1 mm Platte S—G an Luft e	0,578 μ	44°37',4	3°23',2	18,2 μ	34	0,53 μ	1,41	0,2427	
40	1 mm Platte S—G an Luft e	0,578 μ	44°37',4	3°23',2	41,3 μ	34	1,22 μ	3,19	0,2427	
41	1 mm Platte S—G an Luft e	0,578 μ	44°37',4	3°23',2	30,3 μ	34	0,89 μ	2,34	0,2427	
43	1 mm Platte S—G an Luft d	0,578 μ	44°37',4	3°23',2	61,9 μ	62	1,60 μ	2,62	0,2427	
44	1 mm Platte S—G an Luft d	0,578 μ	44°37',4	3°23',2	45,6 μ	60	0,76 μ	2,00	0,2427	
39	½ mm Pl. S—G an Luft e	0,578 μ	44°36',5	3°23',2	33,0 μ	66	0,50 μ	1,31	0,2427	
45	½ mm Pl. S—G an Luft e	0,578 μ	44°36',5	3°23',2	55,3 μ	66	0,84 μ	2,20	0,2427	
46	½ mm Pl. S—G an Luft e	0,578 μ	44°36',5	3°23',2	58,7 μ	66	0,89 μ	2,34	0,2427	
47	½ mm Pl. S—G an Luft e	0,578 μ	44°36',5	3°23',2	56,0 μ	66	0,85 μ	2,23	0,2427	
48	½ mm Pl. S—G an Luft e	0,578 μ	44°36',5	3°23',2	54,1 μ	66	0,82 μ	2,15	0,2427	II
49	½ mm Pl. S—G an Luft e	0,578 μ	44°36',5	3°23',2	52,0 μ	66	0,79 μ	2,07	0,2427	
51	½ mm Pl. S—G an Luft e	0,578 μ	44°36',5	3°23',2	65,7 μ	66	1,00 μ	2,61	0,2427	
52	½ mm Pl. S—G an Luft e	0,578 μ	44°36',5	3°23',2	54,5 μ	66	0,83 μ	2,17	0,2427	
53	½ mm Pl. S—G an Luft e	0 578 μ	44°36',5	3°23',2	49,0 μ	66	0,74 μ	1,95	0,2427	
54	½ mm Pl. S—G an Luft e	0,578 μ	44°36',5	3°23',2	44,0 μ	66	0,67 μ	1,75	0,2427	
55	½ mm Pl. S—G an Luft e	0,578 μ	44°36',5	3°23',2	41,7 μ	66	0,63 μ	1,66	0,2427	
56	1 mm Platte S—G an Luft e	0,578 μ	41°38',2	0°24',0	94,0 μ	37	2,54 μ	6,67	0,0831	
57	1 mm Platte S—G an Luft e	0,578 μ	41°38',2	0°24',0	87,0 μ	37	2,35 μ	6,17	0,0831	
58	1 mm Platte S—G an Luft e	0,578 μ	41°38',2	0°24',0	90,1 μ	37	2,44 μ	6,40	0,0831	
62	1 mm Platte S—G an Luft e	0,578 μ	41°33',6	0°19',4	102 μ	37	2,76 μ	7,24	0,0747	III
63	1 mm Platte S—G an Luft e	0,578 μ	41°33',6	0°19',4	108 μ	37	2,92 μ	7,66	0,0747	
64	1 mm Platte S—G an Luft e	0,546 μ	41°28',6	0°17',7	106 μ	37	2,84 μ	7,88	0,0713	
65	1 mm Platte S—G an Luft e	0,435 μ	41°14',6	0°19',4	68,1 μ	37	1,84 μ	6,46	0,0746	
59	½ mm Pl. S—G an Luft e	0,578 μ	41°37',0	0°23',7	176 μ	74	2,38 μ	6,25	0,0827	
60	½ mm Pl. S—G an Luft e	0,578 μ	41°37',0	0°23',7	172 μ	74	2,32 μ	6,09	0,0827	
77	1 mm Platte S—G an Luft d	0,578 μ	41°27',8	0°13',6	216 μ	62	3,48 μ	9,13	0,0625	
78	1 mm Platte S—G an Luft d	0,578 μ	41°27',8	0°13',6	212 μ	62	3,45 μ	9,05	0,0625	IV
79	1 mm Platte S—G an Luft d	0,578 μ	41°27',8	0°13',6	223 μ	62	3,60 μ	9,45	0,0625	
80	1 mm Platte S—G an Luft d	0,578 μ	41°27',8	0°13',6	221 μ	62	3,56 μ	9,35	0,0625	
81	1 mm Platte S—G an Luft d	0,578 μ	41°27',8	0°13',6	205 μ	62	3,30 μ	8,67	0,0625	
67	1 mm Platte S—G a. Wass. e	0,546 μ	62°38',8	1° 9',8	22,4 μ	17	1,42 μ	3,94	0,1303	
68a	1 mm Platte S—G a. Wass. e	0,578 μ	62°40',5	1° 9',9	36,6 μ	17	2,31 μ	6,06	0,1295	
68b	1 mm Platte S—G a. Wass. e	0,546 μ	62°38',8	1° 9',8	37,4 μ	17	2,36 μ	6,55	0,1303	
69	1 mm Platte S—G a. Wass. e	0,546 μ	62°38',8	1° 9',8	30,5 μ	17	1,93 μ	5,37	0,1303	V
70	1 mm Platte S—G a. Wass. e	0,578 μ	62° 2',1	0°31',5	42,4 μ	17	2,66 μ	6,98	0,0874	
71	1 mm Platte S—G a. Wass. e	0,578 μ	62° 2',1	0°31',5	45,0 μ	17	2,84 μ	7,46	0,0874	
72	1 mm Platte S—G a. Wass. e	0,578 μ	61°49',7	0°19',1	57,5 μ	17	3,61 μ	9,48	0,0681	
73	1 mm Platte S—G a. Wass. e	0,578 μ	61°49',7	0°19',1	60,3 μ	17	3,79 μ	9,95	0,0681	
87 a—f	2 mm Platte S—G an Luft d	0,576 μ	41°27',3	~0°0'						

(Näheres siehe Seite 341 u. Seite 34

Nr. der Aufnahme = Photo No. / Art der Aufnahme = Type of photo

benutzte Hg-Linie = Mercury line used / Gruppe = Group

Platte (or Pl.) = plate / an Luft = to air / a. Wass. = to water

Näheres siehe Seite 341 u. Seite 342 = for details see pp. 15-17 (of present layout)

Table 3

1	2	3	4	5	6	7	8	9	10	11
Nr. der Aufnahme	Art der Aufnahme	benutzte Hg-Linie λ_{Vac}	φ	$\varphi - \varphi_0$	ΔG	Z	ΔD	$\frac{\Delta D}{\Delta\lambda}$	$\sqrt{\sin^2\varphi - \left(\frac{n_2}{n_1}\right)^2}$	Gruppe
11	½ mm Platte, Glas an Luft	Diffz. 0,578 μ — 0,435 μ	44° 36′,5	3° 23′,2 für λ = 0,578 μ	32,7 μ	133	0,246 μ	2,57	0,2427 für λ = 0,578 μ	VI
12	½ mm Platte, Glas an Luft		44° 36′,5		24,6 μ	133	0,185 μ	1,93		
14	½ mm Platte, Glas an Luft		44° 36′,5		24,0 μ	133	0,180 μ	1,88		
15	½ mm Platte, Glas an Luft		44° 36′,5	3° 42′,2 für λ = 0,435 μ	27,5 μ	133	0,207 μ	2,16	0,2537 für λ = 0,435 μ	
16	½ mm Platte, Glas an Luft		44° 36′,5		25,5 μ	133	0,192 μ	2,00		
17	½ mm Platte, Glas an Luft		44° 36′,5		19,5 μ	133	0,147 μ	1,53		
18	½ mm Platte, Glas an Luft		44° 36′,5		34,3 μ	133	0,258 μ	2,69		
19	1 mm Platte, Glas an Luft	Diffz. 0,578 μ — 0,435 μ	44° 37′,5	3° 23′,2 für λ = 0,578 μ	17,0 μ	67	0,254 μ	2,65	0,2427 für λ = 0,578 μ	VII
20	1 mm Platte, Glas an Luft		44° 37′,5		14,5 μ	67	0,216 μ	2,25		
21	1 mm Platte, Glas an Luft		44° 37′,5	3° 42′,2 für λ = 0,435 μ	13,6 μ	67	0,203 μ	2,12	0,2537 für λ = 0,435 μ	
23	1 mm Platte, Glas an Luft		44° 37′,5		12,2 μ	67	0,182 μ	1,90		

Nr. der Aufnahme = No. of photo

Art der Aufnahme = Type of photo

Benutzte Hg-Linie = Mercury line used

Gruppe = Group

½ mm Platte, Glas an Luft = ½ mm plate, glass to air

1 mm Platte, Glas an Luft = 1 mm plate, glass to air

Diff. = difference

für = for

In table 1, n_1 denotes, for the wavelengths $\lambda_{Vac} = 0.578\ \mu$, $\lambda_{Vac} = 0.546\ \mu$, and $\lambda_{Vac} = 0.435\ \mu$, the refractive index in the denser medium (glass) and n_2 that in the less dense medium (air or water).

In tables 2 and 3 (the latter concerns the differential method), all the measurements have been divided into groups (see column 11). The thickness of the reflection plate used in each case is indicated in column 2, "Type of photo". The designation S-G to air, e, for example, means that one side (e) of the plate had a silver strip on the glass (S-G), while d means that there was a silver strip on both sides of the glass, allowing the number of effective reflections to be roughly doubled, although, unfortunately, this usually impaired the quality of the light track on the film. This is why silvering on both sides of the glass was less frequently used. Column 4 gives the angles of incidence of the light beam in the denser medium; it relates to the angular centre of the beam aperture (about 3'). Column 5 lists the corresponding angular distance $\varphi - \varphi_G$ from the critical angle of total reflection, as shown in table 1. Column 6 sets out the ray displacement G actually measured, expressed in μ. Column 7 gives the number Z of effective reflections, column 8 the investigated ray displacement $D = \frac{G}{Z} \frac{\cos \beta'}{\cos \alpha'}$ in the denser medium after one reflection, likewise expressed in μ.

. Columns 6 and 8 in table 3 give the corresponding differential displacements ΔG and ΔD. Finally, column 9 of table 2 gives the values for the ray displacement D in units of wavelength λ_1 for the denser medium, i..e. the values $\frac{D}{\lambda_1}$, and column 9 of table 3 the values $\frac{\Delta D}{\Delta \lambda_1}$, where $\Delta\lambda_1 = \lambda_1$ yellow $- \lambda_1$ blue = 0.096/u. Column 10 is explained in greater detail on pages 19-21. As will be seen from the exposures made with the same $\varphi - \varphi_G$ (groups I and II in table 2 and groups VI and VII in table 3), there is a considerable scatter in the individual values of D, caused by the difficulties of measuring the three-part light track (see figs.3, 5, 9, 10 and 11).

The most remarkable feature of the measurements and of the D values obtained from them is that the D values, i.e. the ray displacements, increase considerably as the critical angle of total reflection is approached (see groups III and IV). Whereas in groups I and II, where $\varphi - \varphi_G = 3^\circ 23.2'$, the mean ray displacement is 0.84/u, this value increases, f.i. in the photos 77-81 (group IV) where the angular distance from critical angle is only 0° 13.6', on the average to 3.48/u or more than fourfold. This fact becomes even more evident in photos 87a-f (see fig. 10), which were taken with 33 effective reflections and a 2 mm plate and for which the apparatus was set as closely as possible to the critical angle of total reflection.

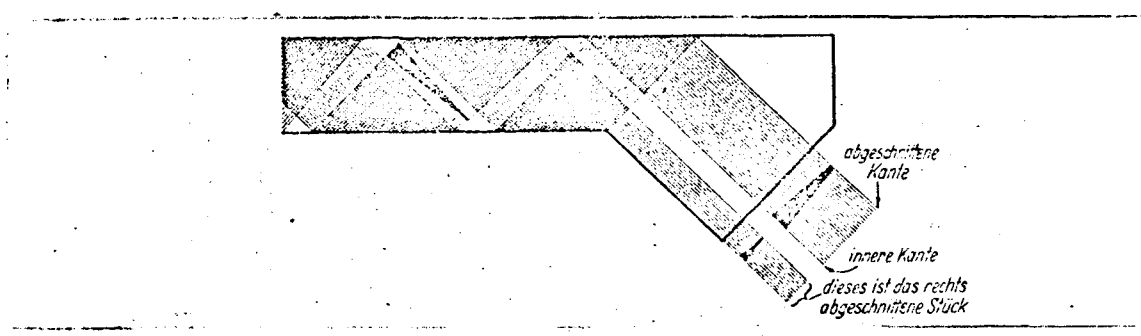

Fig. 8 : Ray path at the limit of total reflection.

Abgeschnittene Kante = cut-off edge ; innere Kante = inner edge

dieses ist das rechts abgeschnittene Stück = this is the part cut off on the right.

Since, however, the aperture angle of the light beam was about 3', part of the beam lies already, of necessity , in the region of partial reflection where it soon becomes invisible owing to the loss of light through multiple reflection. It is only at the very limits of the partial reflection region, where the coefficient of reflection is still close to 1, that some partially reflected light will be recorded on the photographic film. The other, totally reflected part of the beam is considerably broadened and exhibits a peculiar striated structure caused by deflection at slit Sp_2. The left-hand "inner" edge of this light track shows a ray displacement of about 800 μ or, converted to one reflection, a displacement of some 24 μ. The right-hand "outer" edge - - if it can really be called an edge in view of the striated structure - - appears blurred. Only at the very top of this photograph (fig. 10), where the light track is particularly intense, is the right-hand "outer" edge limited by the geometrical configuration of the 2 mm reflection plate used. At best, this plate only allows a light beam some 2.2. mm wide to pass. The part of the track which is cut off on the right, however, reappears on the left, as may be seen from the diagram in fig. 8, and as shown on the photograph in fig. 10, at the point marked "+" for example. It is easy to see that the track fades towards the right and gradually becomes invisible owing to the diminishing intensity of the light. This is indicated in the diagram in fig. 8 by the black wedge.

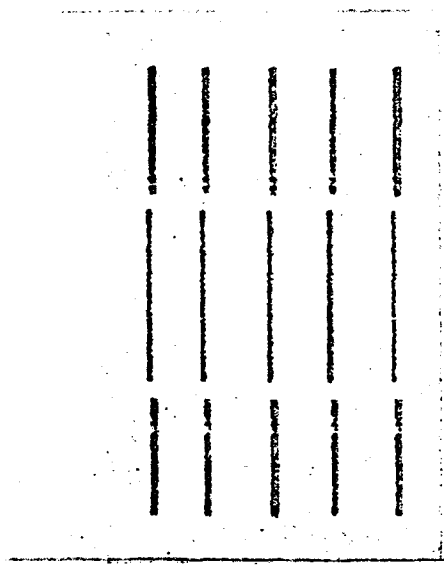

Fig. 9
Enlarged reproduction of photo 64

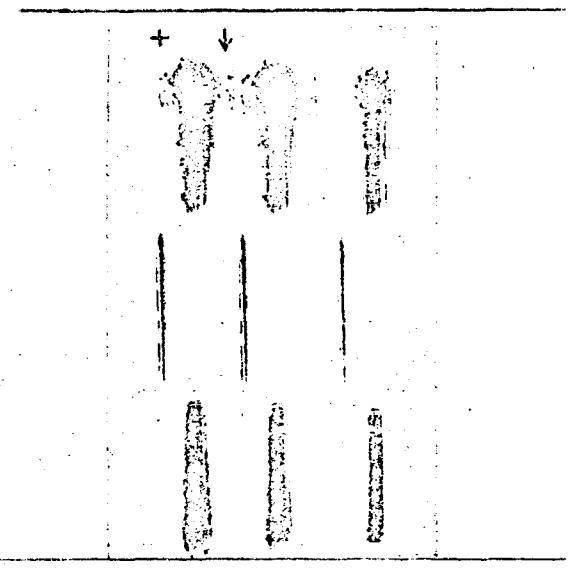

Fig. 10
Ditto for photo 87a

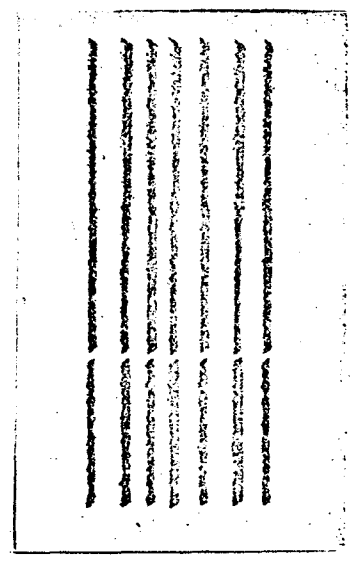

Fig. 11
Enlarged reproduction of photo 18

Between the three individual images in fig. 10, at the point marked with a vertical arrow for instance, other faint striations can be seen which are produced by diffused light, since normally no light can reach these points.

May we point out here, in anticipation of the details set out in §5, that the light track ought to extend from the inner edge to infinity or, in other words, ought to be of infinite width. The outer edge, which would thus lie at infinity, would correspond to that "light ray" of the 3' aperture beam used which coincides precisely with the critical angle of total reflection.

Fig. 9 is a reproduction of photo 64, 3 1/3 times enlarged. It shows five images of the light tracks at $\varphi - \varphi_G = 0^\circ 17.7'$ (see fig. 3 in this connection). The track obtained after total reflection from glass (top and bottom images) is clearly wider than after reflection from silver (central images).

This phenomenon appears in an even more impressive manner in fig. 10. It is explained in detail on pages 16 to 18. Figure 10 is a reproduction of photo 87a, 3 1/3 times enlarged, and shows three images of the light tracks in the immediate vicinity of the critical angle of total reflection.

Fig. 11 is a reproduction of photo 18, $4\frac{1}{2}$ times enlarged. It shows seven images of the light tracks obtained by the differential method (see fig. 5 in this connection) ; the top and bottom series show alternately the colours blue-yellow-blue, etc. while the central one starts with yellow and shows thus the sequence yellow-blue-yellow, etc.

§5. The Function $\sqrt{\sin^2\varphi - \left(\frac{n_2}{n_1}\right)^2}$ and the Constant k

In order to be able to process in a uniform manner the measurements obtained of the ray displacement D which, as shown, give a considerable variation of D with the angular distance $\varphi - \varphi_G$, it is necessary to know the law governing this phenomenon.

Maxwell's theory states that the light energy which enters the less dense medium during total reflection represents a transversely attenuated wave, the amplitude of which decays exponentially with the exponential factor

$$e^{-\frac{2\pi z}{\lambda_1}\cdot\sqrt{\sin^2\varphi-\left(\frac{n_2}{n_1}\right)^2}} \qquad 8)$$

Here, z is the perpendicular distance from the boundary surface, λ_1 the wavelength in the denser medium (hence $\lambda_1 = \frac{\lambda_{Vac}}{n_1}$), φ the angle of incidence in the denser medium, n_1 the refractive index of the denser medium and n_2 that of the less dense medium.

The transverse attenuation of the movement of the light in the less dense medium produces a so-called "depth of penetration" of the totally reflected light into the less dense medium. The phenomenon of the ray displacement D must be directly related to this depth of penetration. In fact, it was possible to represent the value D for all the results observed uniformly by $D = k \cdot n_2 \cdot \frac{\lambda_1}{\sqrt{\sin^2\varphi-\left(\frac{n_2}{n_1}\right)^2}}$, (1) where k is a dimensionless constant. Hence, the exponential factor of Maxwell's theory may also be written in the form $e^{-2\pi k \cdot n_2 \cdot \frac{z}{D}}$.

This constant k, $k = \frac{D}{\lambda_1}\cdot\frac{1}{n_2}\cdot\sqrt{\sin^2\varphi-\left(\frac{n_2}{n_1}\right)^2}$ (2) was derived from the observations, i.e. in a purely empirical manner. The relevant values of $\sqrt{\sin^2\varphi-\left(\frac{n_2}{n_1}\right)^2} = \sqrt{\sin^2\varphi-\sin^2\varphi_0}$ are set out in column 10 of tables 2 and 3.

As φ approaches φ_0, this root decreases, at first slowly, then very rapidly just before the critical angle is reached, i.e. when φ is very close to φ_G. Consequently, the ray displacement D increases at first slowly, and then rapidly as the critical angle comes very close, as shown in fig.10.

If it were possible to work with an energy-carrying light beam of zero aperture angle, observation would show that, as the critical angle of total reflection is approached more and more closely, the ray displacement D continues to increase, becoming infinitely large at the critical angle itself. This means, however, that here, i.e. in the border-line case, the light energy which has entered the less dense medium would travel along the boundary surface into infinity. According to Maxwell's theory, the wave in this extreme case would be homogeneous and no longer transversely attenuated.

The most probable value for the constant $\underline{k}$ was determined in the following way from all the observations made : In groups I and II in table 2, where all photos were made with the same value of $\varphi - \varphi_G$, the arithmetic mean of all (identically weighted) D values was calculated for each group and the corresponding value of $\underline{k}$ derived therefrom by means of equation 2 (page 20). The same procedure was used for the differential photos of groups VI and VII (table 3) ; the mean values $\Delta D = D_{yellow} - D_{blue}$ were found (see figs. 5 and 11) and $\underline{k}$ was again calculated from

$$k = \frac{\Delta D}{\left(\frac{\lambda_1 \cdot n_2}{\sqrt{\sin^2\varphi - \left(\frac{n_2}{n_1}\right)^2}}\right)_{gelb} - \left(\frac{\lambda_1 \cdot n_2}{\sqrt{\sin^2\varphi - \left(\frac{n_2}{n_1}\right)^2}}\right)_{blau}} \qquad (3)$$

(gelb = yellow, blau = blue).

For the photos of groups III, IV and V (table 2), on the other hand, $\underline{k}$ was calculated from D for each individual photo and the mean of $\underline{k}$ established within each group. These group means are set out in table 4.

Gruppe	k	wahrscheinl. Fehler w in % von k	Gewichte $p \sim \frac{1}{w^2}$	Gruppe	k	wahrscheinl. Fehler w in % von k	Gewichte $p \sim \frac{1}{w^2}$
I	0,564	± 7,9%	1	V	0,510	± 3,5%	5
II	0,505	± 3,2%	6	VI	0,451	± 5,2%	2
III	0,537	± 1,5%	28	VII	0,478	± 4,9%	3
IV	0,553	± 1,7%	22				

Table 4

Gruppe = Group Gewichte = Weightings

wahrscheinl. Fehler w in % von k = probable error w as a percentage of k

It will be seen that the differential photos (groups VI and VII) give a lower value for k.

The probable percentage error w within each group is set out in column 3 of the table, while column 4 lists the weightings $p \sim \frac{1}{w}2$ which were used to calculate the general mean for the groups I - VII. The following result was obtained:

$$k = \frac{\Sigma(k.p)}{\Sigma p} = 0.533 \pm 1.1\% \text{ (probable percentage error).}$$

The probable error w shows extreme variations among the individual groups ; it is relatively small for groups III and IV because the ray displacement D is here already fairly large, hence the percentage accuracy of the measurement high. It must be emphasized, however, that in the case of groups III and IV, where the values $\varphi - \varphi_G$ are already of the order of minutes of arc, an error of as little as half a minute in the angular setting (the accuracy with which the vernier scale can be read) is quite noticeable. Thus, for example, for $\varphi - \varphi_G = 15'$, an error $\Delta(\varphi - \varphi_G)$ of $\frac{1}{2}'$ can produce an error of more than 3% in the factor $\sqrt{\sin^2\varphi - \sin^2\varphi_G}$.

In view of this, the procedure of finding a mean with such divergent weightings does not seem justified. If, however, the mean of groups I - VII is calculated with the same weighting for all seven groups, the result is k = 0.514 $\pm$ 2.1% (probable error).

A further attempt at establishing the mean was made by calculating the value of $\underline{k}$ for each individual photo, i.e. without any grouping, and taking the mean with identical weightings. This gave the value

$$k = 0.519 \pm 1.8\% \text{ (probable error)}$$

so that the use of

$$k = 0.52 \pm 2\ \% \text{ (probable percentage error)}$$

as a general mean for $\underline{k}$ seems justified. If $\varphi - \varphi_G$ is now calculated from equation (1) for the "inner" edge of the light track in photo 87a, using the above value for $\underline{k}$ and the measured displacement D (see page 20 and fig. 10), the result is $\varphi - \varphi_G = 13''$; this means that by far the major part of the 3'-aperture beam was, in fact, already situated in the region of partial reflection.

Addendum during proof-reading

The experiments were repeated during the winter of 1943/44, using the differential method and polarized light.

The results were :

electrical vector perpendicular to the plane of incidence:

$D = 0.230/u$;

electrical vector parallel to the plane of incidence:

$D = 0.231/u$; or, in other words, there was no difference.

From this, constant $\underline{k}$ was calculated at k = 0.52.

Hamburg, State Institute for Physics, 25.10.1943

Footnotes

1) W. Voigt : Ann.Physik 67, 185 (1899)

A. Eichenwald : J. Russ.Phys.-chem. Soc.Phys.Sect. 41, 131 (1909)

J. Picht : Ann. Physik 3, 433 (1929)

F. Noether : Ann. Physik 11, 141 (1931)

For comprehensive survey see e.g. :

v. Laue : Handb. d. Experimentalphysik (Experimental Physics Handbook), vol. XVIII, pp. 150 et seq.

W. König; Handb. d. Physik, Bd XX, pp. 228 et seq.

Clemens Schaefer : Einführung in die theoretische Physik (Introduction to theoretical physics), vol. III, 1, pp. 406 et seq.

2) I. Newton : Optice, Liber secundus, Observatio 1.

3) Comprehensive survey as in footnote 1), where the individual bibliographical references are likewise set out

4) F. Goos and H. Hänchen : Ann. Physik 43, 383 (1943)

5) W. Voigt : Ann. Physik 67, 185 (1899)

6) P. Selenyi : C.R. Acad. Sci. Paris 157, 1408 (1913)

7) F. Goos : Z. Physik 100, 95 (1936)

8) e.g. Clemens Schaefer : Einführung in die theoretische Physik (Introduction to theoretical physics), vol. III, 1, p. 414